

# Wind tunnel experiments of a building model incorporating viscous-damping walls

Austin D.E. Pan<sup>†</sup>

*Department of Civil Engineering, The University of Hong Kong, Pokfulam Road, Hong Kong, S.A.R.*

Ngai Yeung<sup>‡</sup>

*Ove Arup & Partners Hong Kong Ltd., Level 5, Festival Walk, Tat Chee Avenue, Kowloon Tong, Hong Kong, S.A.R.*

**Abstract.** This paper presents an experimental study on the effectiveness of viscous-damping walls in controlling the wind-induced vibrations of a building model. A simple four-story building model, square in plan, was constructed for wind tunnel study. In this paper the description of the model, its instrumentation, and the experimental set-up and methodology are reported. The effectiveness of viscous-damping walls in reducing vibrations was investigated for different fluid levels in the walls, and at varying wind speeds and attack angles. The results show that viscous-damping walls are highly effective in most cases.

**Key words:** viscous-damping wall; wind tunnel experiment; wind-induced vibration; vibration control.

---

## 1. Introduction

The trend toward higher and more flexible buildings has produced structures that often lack sufficient inherent damping and are more sensitive to wind excitations. The dynamic aspect of wind loading may cause discomfort to building occupants which presents a serviceability issue. A fundamental way of controlling wind-induced vibrations is to incorporate a significant level of damping within structures. Passive control devices may be used for this purpose. This paper reports an experimental study on a passive control device referred to as the *viscous-damping wall*.

A Japanese engineer, Mitsuo Miyazaki, first proposed the concept of viscous-damping wall in the 1980s as a form of passive vibration control device that would substantially increase the inherent damping of buildings and thus reduce dynamic response (Miyazaki *et al.* 1986). In 1992 the Media City Shizuoka Building, the first building incorporating viscous-damping walls in the world, was constructed at the center of Shizuoka city, 150 km west of Tokyo. This 78-meter high steel-frame building had 170 viscous-damping walls installed (Miyazaki and Mitsusaka 1992). After construction, damping values of up to 27% (at 20°C) for the first mode were measured by investigators (Miyazaki and Mitsusaka 1992). There are a number of other buildings in Japan that have incorporated viscous-damping walls (PSRG 1997) for the main purpose of seismic resistance. There has been scant

---

<sup>†</sup> Associate Professor

<sup>‡</sup> Civil Engineer

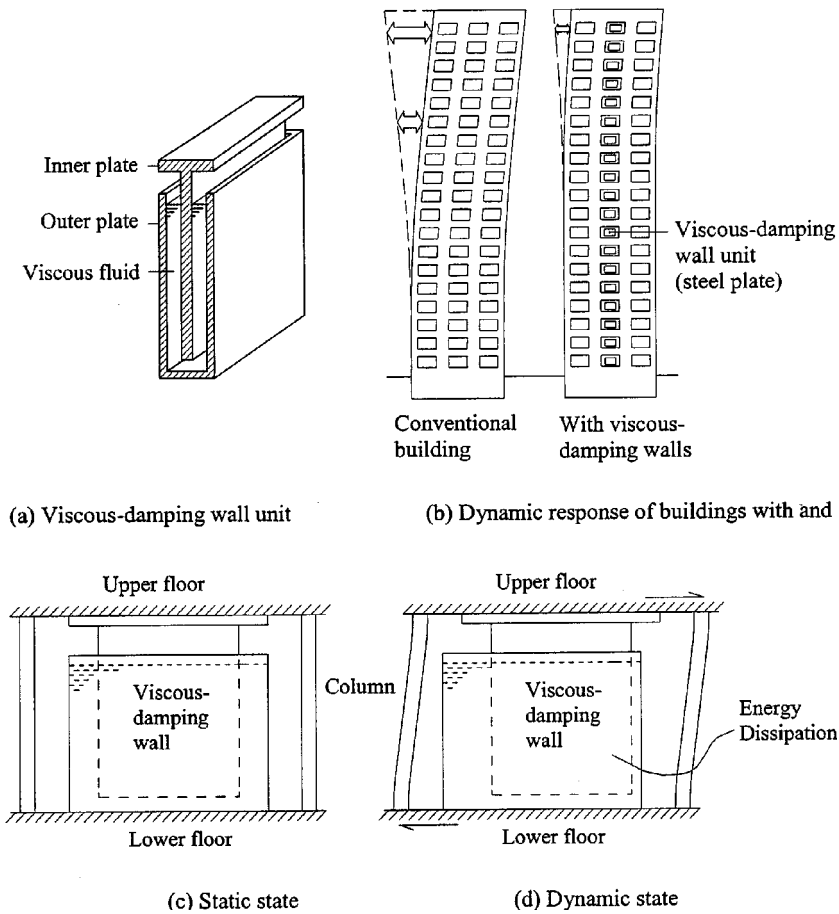


Fig. 1 Viscous-damping wall

research in the use of viscous-damping walls for reducing wind-induced vibrations.

The basic viscous-damping wall unit, illustrated in Fig. 1(a), consists of high-viscosity fluid sandwiched by three wall plates. The inner plate is attached to the upper floor of a building story while the two outer plates are mounted on the lower floor, as shown in Fig. 1(c). When a building is subjected to dynamic forces induced by earthquake or wind, each story will experience relative horizontal displacements between the upper and lower floors (Fig. 1(d)). This inter-story drift causes the inner plate to move relative to the outer plates. This action, due to the presence of the viscous fluid between the plates, generates viscous-damping forces that oppose the inter-story drift. The overall dynamic response of the building is thereby reduced (Fig. 1(b)).

Test results of preliminary building models incorporating viscous-damping walls have been previously reported by the authors (Yeung and Pan 1997 and 1998). Our program of wind tunnel experiments for viscous-damping walls is believed to be the first ever conducted. This paper presents a more comprehensive study of a new building model in which the scaling has been selected to produce a larger vibrational response due to vortex shedding. The model was subjected to five series of wind tunnel tests in which the height of the viscous fluid added varied from 0 to full. In each series of test, wind velocity was incremented in five steps, from 6 m/s to 14 m/s, and

the angle of wind attack varied from 0 to 90 degrees.

## 2. Damping mechanism

The viscous-resistant force ( $Q_w$ ) generated in the viscous-damping wall can be expressed by the Voight-Kelvin model (Miyazaki *et al.* 1986) as follows

$$Q_w = Q_c + Q_k \quad (1)$$

where  $Q_c$  is the damping force due to the velocity gradient in the fluid and  $Q_k$  is the restoring force due to the relative displacement between the wall plates.

The formula for the damping force  $Q_c$  may be expressed as

$$Q_c = \mu A \left( \frac{dv}{dy} \right)^\alpha \quad (2)$$

where  $A$  is the area of the plate,  $\mu$  is the fluid viscosity,  $dv$  is the relative velocity, and  $dy$  is the gap distance between the plates (see Fig. 2). Since the viscous fluid used in viscous-damping walls is usually not a perfect Newtonian fluid, an exponent factor  $\alpha$ , which is obtained from experiments, is applied to the term  $dv/dy$ .

Based on a series of cyclic testing of viscous-damping walls, an empirical equation for  $Q_c$  was obtained by Miyazaki *et al.* (1986)

$$Q_c = 0.59 \cdot e^{-0.043t} \cdot A \cdot \left( \frac{dv}{dy} \right)^{0.5} \quad (3)$$

where  $t$  is the temperature of the viscous fluid. Eq. (3) shows that  $Q_c$  decreases with increase in temperature.

The restoring force  $Q_k$ , which is dependent on the relative displacement between plates, may be expressed as (Arima *et al.* 1988)

$$Q_k = \mu A \frac{\delta^\beta}{dy^2} \quad (4)$$

where  $\delta$  is the relative displacement and the exponent factor  $\beta$  is obtained from experiments.

For the viscous-damping walls they tested, Arima *et al.* obtained the following empirical expression for  $Q_k$

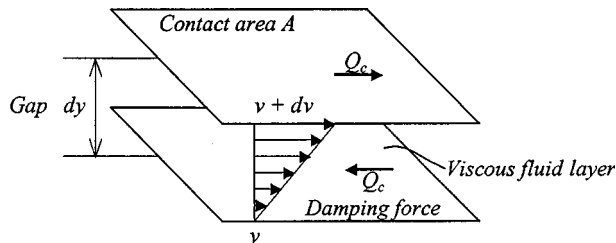


Fig. 2 Principle of viscous-damping

$$Q_k = a_r K \delta \quad (5)$$

where

$a_r$  : modification factor for displacement (see appendix)

$K$  : reference stiffness matrix index defined as (see appendix for expression of terms) :

$$K = 0.9 \times a \times \mu \times f^{0.5} \times A / dy \quad (6)$$

### 3. Description of the building model

An aeroelastic building model incorporating viscous-damping walls was designed and constructed for testing in the wind tunnel at the University of Hong Kong. The model was first tested without viscous fluid and then with various levels of fluid so that the behavior and effectiveness of viscous-damping walls could be compared.

An elevation view of the finished four-story building model, with viscous-damping walls installed, is shown in Fig. 3 (exterior cladding removed). Overall dimensions of the test model are 330-mm by 330-mm in plan and 1200-mm in height. The floor slabs and wall plates were made of perspex and the columns of stainless steel. The diameter of the column is 8 mm, and the thickness of walls and floor slabs are 6 mm and 10 mm, respectively. A single viscous-damping wall unit was installed at the center of each floor.

The four-story aeroelastic building model was constructed at 1:12 scale. Appropriate velocity and other aeroelastic scales were selected so that the wind flow around the model would be similar to

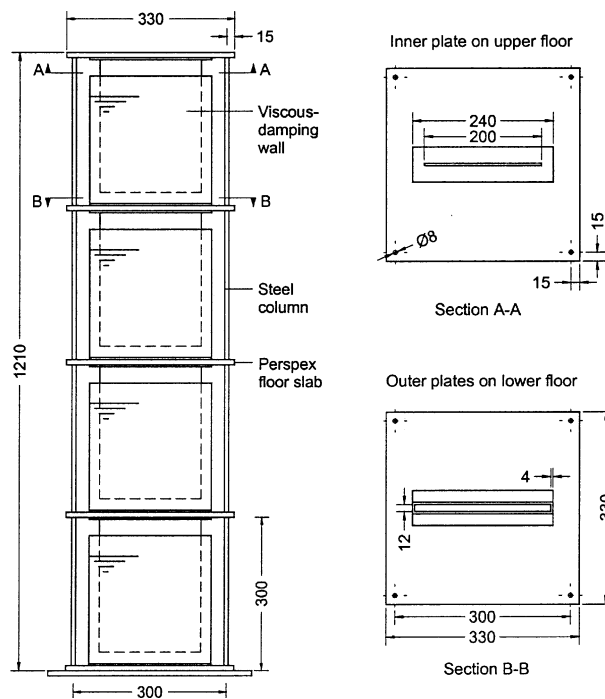


Fig. 3 Dimensions of the building model

Table 1 Aeroelastic scaling

Property	Modeling parameter	Scale value
Length	$L_m / L_p$	1/12
Velocity	$V_m / V_p$	1/5
Time	$T_m / T_p = V_p L_m / V_m L_p$	5/12
Acceleration	$a_m / a_p = V_m^2 L_p / V_p^2 L_m$	12/25
Material density	$\rho_m / \rho_p$	1
Air density	$\rho_{air\ m} / \rho_{air\ p}$	1
Mass	$m_m / m_p = \rho_m L_m^3 / \rho_p L_p^3$	1/1728
Frequency	$N_m / N_p = T_p / T_m$	2.4
Mass moment of inertia	$J_m / J_p = \rho_m L_m^5 / \rho_p L_p^5$	4.02E-06
Stiffness	$K_m / K_p = \rho_m L_m^3 T_p^2 / \rho_p L_p^3 T_m^2$	1/300
Moment of inertial	$I_m / I_p = K_m L_m^3 / K_p L_p^3$	1.93E-06
Force	$F_m / F_p = \rho_m L_m^4 T_p^2 / \rho_p L_p^4 T_m^2$	2.78E-04
Moment	$M_m / M_p = \rho_m L_m^5 T_p^2 / \rho_p L_p^5 T_m^2$	2.31E-05
Damping	$\zeta_m / \zeta_p$	1

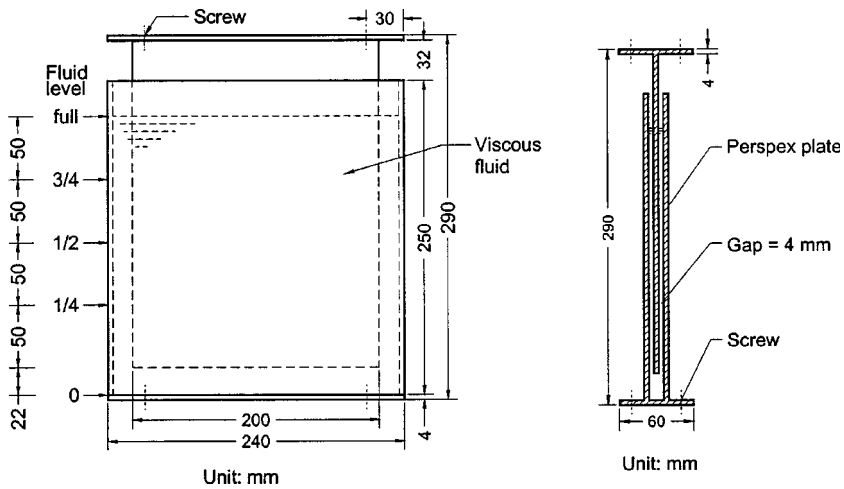


Fig. 4 Dimensions of the viscous-damping wall unit

the wind around the assumed prototype building. The scaling factors are given in Table 1. We adopted an aeroelastic design for the model because it could provide the best information on the response of a flexible building structure such as displacements, rotations and accelerations. Aeroelastic measurements were carried out at several wind speeds, selected to simulate a representative range of full-scale wind.

A detailed drawing of the viscous-damping wall unit is shown in Fig. 4. The overall dimensions of the wall unit installed in the building model is 240-mm in width and 290-mm in height. The gap distance between the inner plate and outer plates is 4 mm. The fluid used to fill the wall units was silicone (Jaeger 1408s) with a viscosity of 12,000 centistokes and density of 974 kg/m<sup>3</sup> at 25°C. Silicone is a clear, colorless, and odorless fluid. It is bland, chemically inert, and non-corrosive to

Table 2 Material properties

Property	Column	Wall plate	Floor slab	Viscous fluid
Material	Steel	Perspex	Perspex	Silicone
Density (kg / m <sup>3</sup> )	6780	1225	1225	974
Geometry (mm)	$d^{(1)} = 8$	$t^{(2)} = 4$	$t^{(2)} = 10$	
Material property	$f_y^{(3)} = 668$	–	–	$\mu^{(4)} = 12,000$

<sup>(1)</sup> $d$  : diameter, <sup>(2)</sup> $t$  : thickness, <sup>(3)</sup> $f_y$  : yield stress (MPa), <sup>(4)</sup> $\mu$  : viscosity at 25°C (centistoke)

most construction materials. Another advantage of silicone fluid is that it is available at a wide range of viscosity levels (e.g., 5 to 500,000 centistokes). In actual buildings where full-scale viscous-damping walls are installed, polybutane has been the choice in most cases for the viscous fluid.

The material properties used to construct the model are summarized in Table 2. The net weight of the finished model was 20.0 kg (excluding the weight of the viscous fluid, added mass and instrumentation). According to the aeroelastic modeling the total weight of the model should equal to 30.6 kg for the assumed prototype building. Therefore, added mass in the form of brass blocks was added to each floor so that the total model weight was near 30 kg in total.

A full description of the building model, together with the experimental set-up and results, can be found in the doctoral thesis by Yeung (2000).

#### 4. Experimental set-up

##### 4.1. Wind tunnel

A schematic diagram of the wind tunnel with model and set-up is shown in Fig. 5. The working section of the wind tunnel at the University of Hong Kong is 3-m wide and 1.8-m high and 18 m in length. The 2-m diameter wind fan can produce a maximum air-stream speed of 18 m/s. A grid of

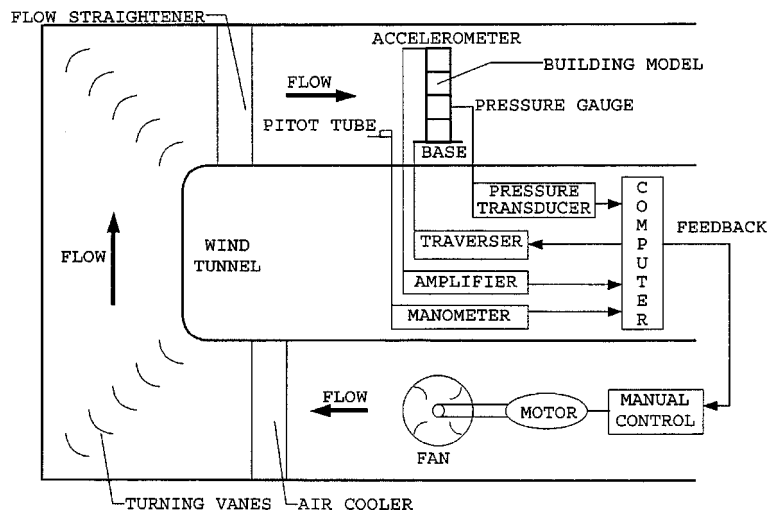


Fig. 5 Schematic wind tunnel testing

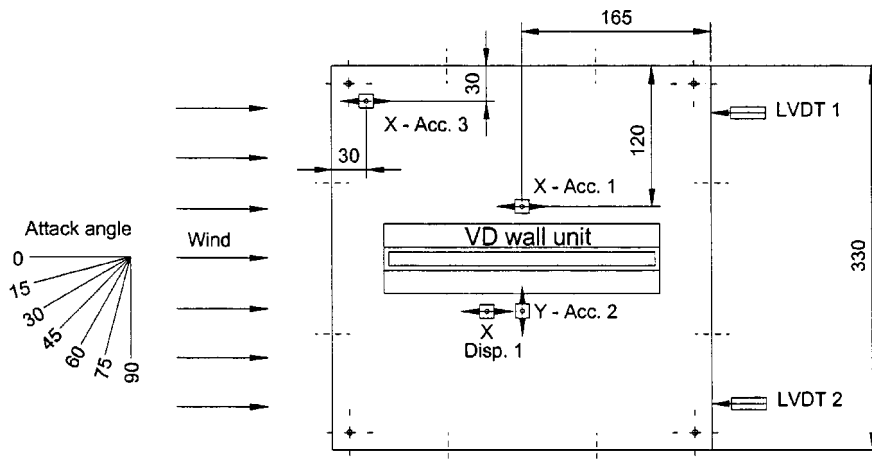


Fig. 6 Instrumentation

wood blocks covers the floor of the wind tunnel to simulate ground friction. The tunnel is equipped with a Pitot tube, on a variable positioning control, and a 3-m diameter rotating base on which the viscous-damping building model was placed. The temperature in the wind tunnel was controlled at a constant 25°C.

#### 4.2. Instrumentation of the building model

A total of 32 channels of data were recorded during each test. To measure dynamic response, the model was instrumented with piezoelectric accelerometers oriented in both  $x$ - and  $y$ -axis directions (see Fig. 6). On each floor, including the roof, two accelerometers (PCB model 352B68) were mounted near the center to measure translational accelerations. Another accelerometer was installed near the corner of the floor. In addition, a displacement meter (B&K 4370/4371 with amplifier 2635) was installed near the center of each floor to measure the major-axis displacement. And externally, two displacement transducers (LVDTs) were installed to measure absolute horizontal displacements at the roof level.

The average wind velocity was measured using the Pitot tube in the test section of the wind tunnel. Pressure gauges were placed on the exterior cladding of the model to obtain wind pressure profiles.

Force transducers (PCB Piezotronics 208B02) were installed at the base of each steel column of the model to measure axial forces.

All sensors and their corresponding signal conditioners were calibrated prior to testing. Signals were filtered and amplified before transfer to the computer for display and storage. The signals were sampled and analyzed using the Global Lab software package with an A/D data acquisition board (DT 709Y & DT 752). The feedback of the measured data was used to adjust wind tunnel operating and the testing process.

### 4.3. Testing

#### 4.3.1. Pre-tests

Before wind tunnel testing commenced, the dynamic properties of the model were measured. These included stiffness, natural frequencies, mode shapes, and equivalent viscous damping ratios.

A force-displacement test was conducted to determine the lateral stiffness of the model. A maximum static lateral load of 5 N was applied at 1-N increments. After each 1-N increment, approximately one minute was allowed to elapse for the model to reach a static state. Then the

Table 3. Wind tunnel testing program and results

Test series	Fluid level (see Fig. 4)	Test No.	Wind attack angle (see Fig. 6)	Peak acceleration (m/s <sup>2</sup> )	Peak displacement (mm)
1	0	1	0 degree	1.74	1.16
		2	15	0.51	1.15
		3	30	0.67	1.07
		4	45	0.44	0.72
		5	60	0.41	0.74
		6	75	0.41	0.79
		7	90	0.53	2.72
2	1/4	8	0	1.38	1.04
		9	15	0.51	0.91
		10	30	0.43	0.85
		11	45	0.43	0.73
		12	60	0.44	0.57
		13	75	0.40	0.71
		14	90	0.49	2.50
3	1/2	15	0	1.33	0.77
		16	15	0.43	0.64
		17	30	0.43	0.66
		18	45	0.43	0.56
		19	60	0.37	0.39
		20	75	0.38	0.44
		21	90	0.46	1.62
4	3/4	22	0	1.05	0.63
		23	15	0.43	0.47
		24	30	0.35	0.47
		25	45	0.36	0.39
		26	60	0.38	0.35
		27	75	0.38	0.36
		28	90	0.45	1.61
5	Full	29	0	1.03	0.49
		30	15	0.39	0.36
		31	30	0.38	0.36
		32	45	0.39	0.26
		33	60	0.36	0.29
		34	75	0.36	0.33
		35	90	0.45	1.11

lateral displacements were recorded by two LVDTs. Upon unloading, the same testing procedure was followed. The average lateral stiffness of the model was thus determined to be 1320 N/m.

After the model was installed on the testing platform in the wind tunnel, free vibration tests were conducted by the pull-back method. An initial horizontal displacement of approximately 10 mm was imparted at the roof level and then the model was released. Based on the recorded response, damping ratios were computed and are reported in Section 5.1.

#### 4.3.2. Wind tunnel tests

The wind tunnel testing program is summarized in Table 3. The main variables selected for the testing program were:

- (1) fluid level
- (2) wind velocity
- (3) wind attack angle

A total of 35 tests were carried out, grouped into five series according to the level of fluid in the viscous-damping walls. The fluid level varied, as marked in Fig. 4, from 0 in Test Series 1 to full-height in Test Series 5.

The duration of each of the 35 tests was approximately 9 minutes during which the model experienced 5 different levels of wind velocity. The target wind velocity history is shown in Fig. 7. Starting off at approximately 6 m/s, the target wind velocity was increased to 8 m/s. After about one minute, the wind velocity was reduced back to 6 m/s. This cycle of loading was repeated for higher target wind velocities of 12 m/s and 14 m/s. The latter velocity, according to our modeling, simulates an extreme case of wind loading of 252 km/hour.

In real situations the wind blows onto buildings from all directions. The influence of wind direction was simulated in the test program. Each test series consisted of seven sequences of tests for different wind attack angles (see Table 3 and Fig. 6). The turntable in the wind tunnel was rotated, at 15-degree increments, starting from 0 degree in the first test sequence to 90 degrees in the last sequence.

## 5. Results

The acceleration and displacement histories, root-mean-square (RMS) accelerations, and acceleration

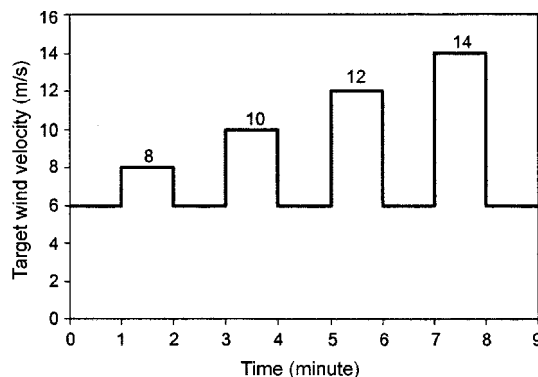


Fig. 7 Wind velocity history for the wind tunnel testing

response spectra were among the measures used to evaluate the effectiveness of viscous-damping walls, as well as the influences of wind attack angle and fluid level.

### 5.1. Free vibration tests

From the results of the free vibration tests of the building model, damping values were computed to be about 4% for the case of no viscous fluid to 20% after the viscous-damping walls were fully filled. Damping values in this range have been reported in actual buildings where full-scale viscous-damping walls were installed (Miyazaki and Mitsusaka 1992). A plot of damping versus fluid level is shown in Fig. 8. The relationship is nonlinear. There is a large increase in damping when the fluid level increases from zero to 1/4. Above the 1/4 level, the increase in damping is not as substantial. Fig. 9 shows a typical response history from the free vibration tests.

The power spectra of model response for the no-fluid case and for the half-fluid case are shown in Fig. 10. Without viscous fluid, the fundamental natural frequency of the test model was 2.15 Hz,

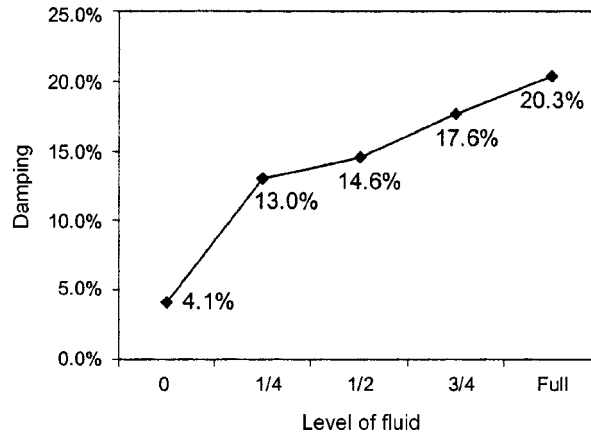


Fig. 8 Structural damping of model

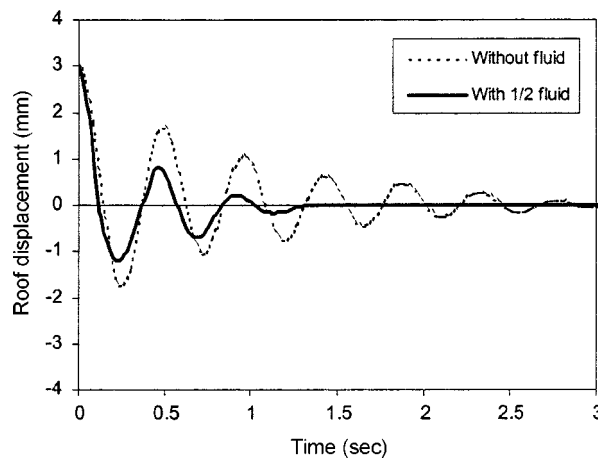


Fig. 9 Free vibration decay curve of the roof

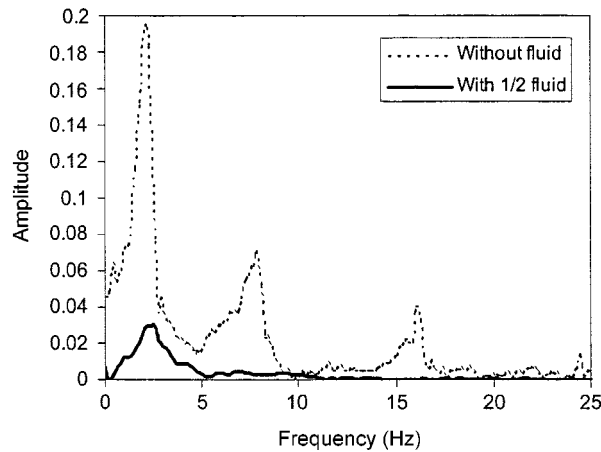


Fig. 10 Power spectra of the model response

and the frequencies of the successive modes were 7.82 Hz, 16.24 Hz and 24.45 Hz. After the walls were half-filled with viscous fluid the fundamental natural frequency increased to 2.35 Hz. And at full-fluid the fundamental frequency shifted to 2.74 Hz. We believe this increase in frequency is primarily the result of the additional stiffness provided by the viscous-damping walls. Fig. 10 depicts how highly damped the model becomes after fluid is added, with the higher frequencies of vibration hardly detectable.

### 5.2. Along-wind response

During wind tunnel testing, due to the influence of turbulence with each change in wind velocity, the model without viscous fluid vibrated very vigorously in both the translational and torsional modes. After viscous fluid was added, we observed a remarkable improvement in the response of the model. After each change in wind speed the viscously-damped model deflected in a gradual and controlled manner toward a new equilibrium position; vibrations in both the translational and torsional modes were hardly perceptible.

Fig. 11 shows a typical wind pressure history taken from the windward pressure gauge on the third-floor cladding of the model. Figs. 12 and 13 are the along-wind acceleration histories measured at the roof level. When the wind velocity was below 8 m/s the difference in response between the no-fluid and full-fluid cases was not significant. But at higher wind speeds the model without viscous fluid experienced more severe vibrations compared with the model with viscous fluid, about two times in terms of accelerations. Only in the last phase of the response history, when the wind velocity was at the extreme condition of 14 m/s, did the viscously-damped model experienced fairly significant vibrations.

The reduction in vibration after adding viscous fluid was even more evident from the measured displacements. Figs. 14 and 15 show the displacement histories recorded on the roof. A comparison between the no- and full-fluid cases shows that the reduction in displacement was on the order 60% to 80%.

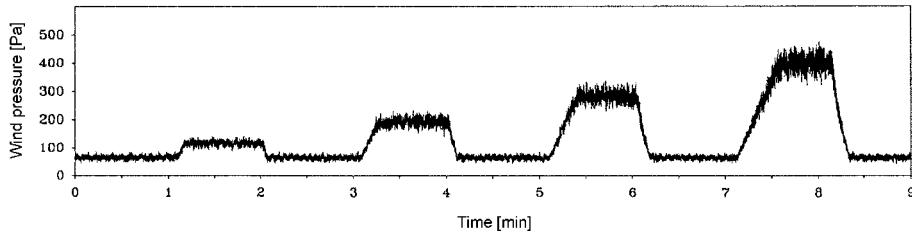


Fig. 11 Wind pressure history on the front panel of the model at 3/F

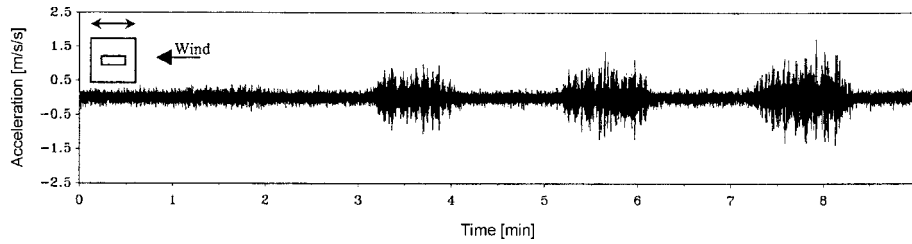


Fig. 12 Along-wind acceleration at roof: no fluid case

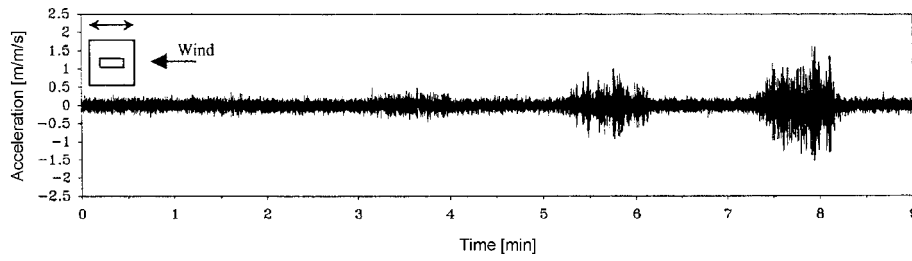


Fig. 13 Along-wind acceleration at roof: full fluid case

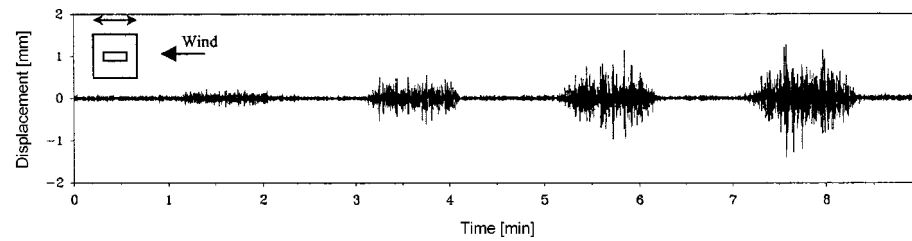


Fig. 14 Displacement at roof: no fluid case

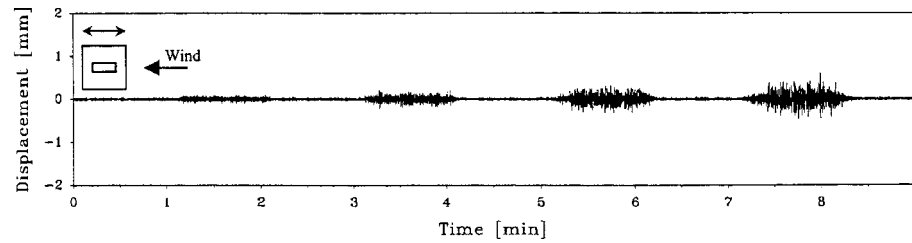


Fig. 15 Displacement at roof: Full fluid case

### 5.3. Cross-wind response

The wind tunnel tests showed that even when the viscous-damping wall units were aligned in the along-wind direction, the viscous damping helped to reduce the response of the model in the cross-wind direction. At the wind attack angle of 0 degree, the viscous-damping walls reduced the cross-wind displacements by at least 40% (see Figs. 16 and 17). As seen in Fig. 16, the cross-wind displacements were fairly significant in all phases of wind speed. Comparatively, this situation was improved after the addition of viscous fluid (Fig. 17). Cross-wind displacements were only significant during the last phase of wind speed.

### 5.4. Acceleration response spectra

The response spectra of the model with and without viscous fluid are shown in Figs. 18 and 19 for response in the along- and cross-wind directions, respectively. These were obtained by the power transform (FHT) of the recorded accelerations at the roof level. It is evident that wind-induced vibration was effectively dissipated by the viscous-damping wall units. Both spectra also show a shift of the first mode of vibration after fluid was added. As previously noted, this is likely due to the increased stiffness provided by the viscous-damping walls.

### 5.5. Effect of wind attack angle

In real situations, wind attacks a building from all possible directions. To model these situations in the wind tunnel, the turntable was rotated in the clockwise direction (so that the direction of wind would change in the anti-clockwise direction, see Fig. 6). Figs. 20 and 21 show how varying the wind attack angle affects the dynamic response of the model and the effectiveness of the viscous-damping walls. The root-mean-square (RMS) of acceleration response measured at roof level is

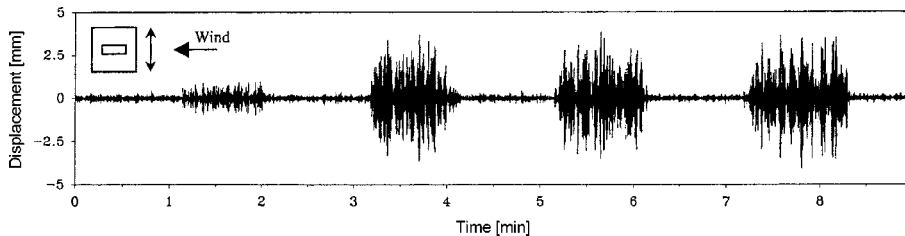


Fig. 16 Cross-wind displacement at roof: no fluid case

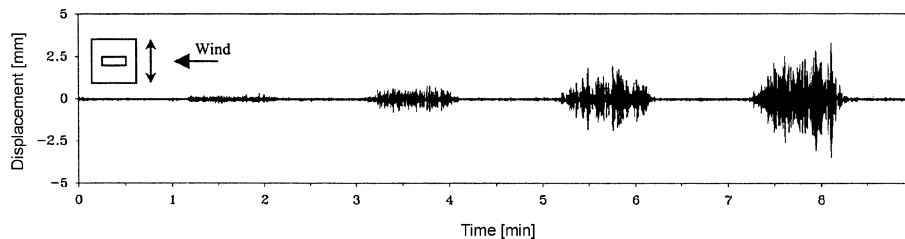


Fig. 17 Cross-wind displacement at roof: full fluid case

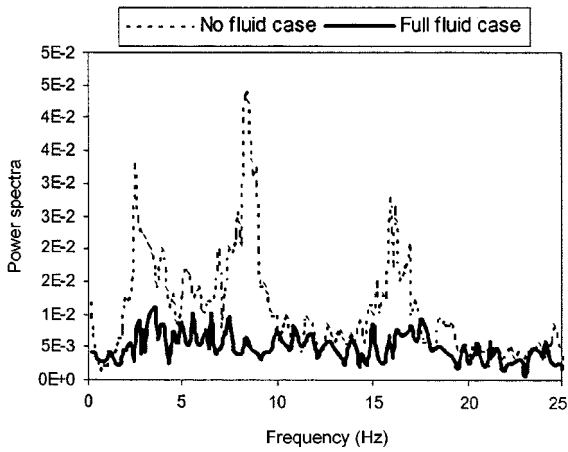


Fig. 18 Along-wind response spectra of the model

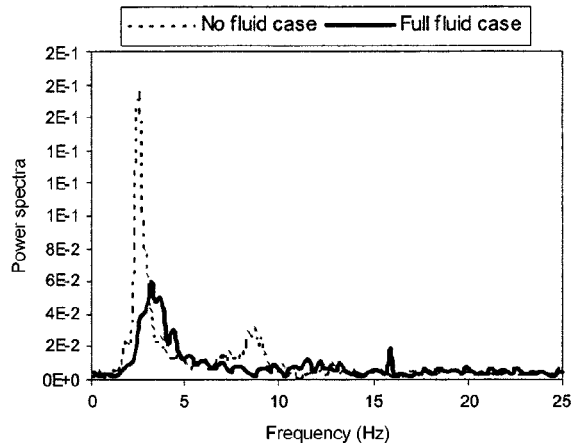


Fig. 19 Cross-wind response spectra of the model

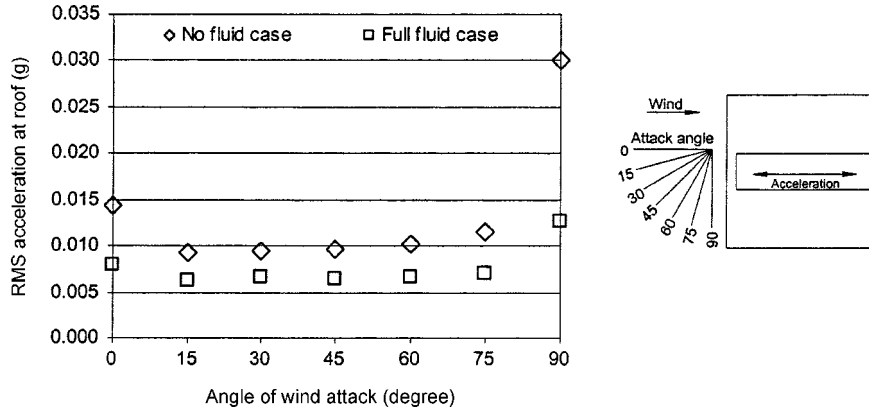


Fig. 20 Root-mean-square acceleration of the model: in-plane direction of the viscous-damping wall

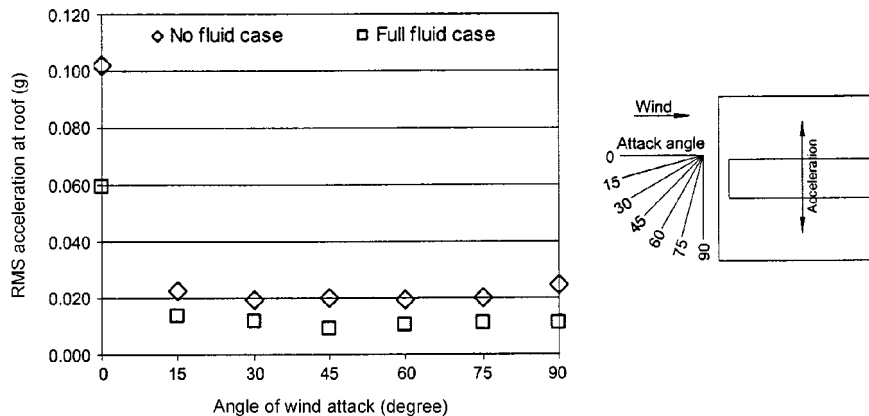


Fig. 21 Root-mean-square acceleration of the model: out-of-plane direction of the viscous-damping wall

plotted against 15-degree increments of wind angle. Due to the influence of vortex shedding, the maximum response occurs when the direction of wind is normal to the face of the building (i.e., angle of wind attack equal to 0 or 90 degrees). At these two critical directions Figs. 20 and 21 show that the viscous-damping walls are most effective. But even at other wind angles, the viscous-damping walls remained highly effective in suppressing wind-induced accelerations. Figs. 20 and 21 are from results of a target wind speed equal to 12 m/s (which is equivalent to a full-scale wind speed of about 60 m/s, the level for a 50-year return period in Hong Kong). At other target wind speeds, the results for the effectiveness of the viscous-damping walls showed a similar pattern.

## 6. Conclusions

This paper reports on what are believed to be the first ever wind tunnel studies of an aeroelastic building model incorporating viscous-damping walls. The purpose of the study was to investigate the behavior and effectiveness of viscous-damping walls in controlling wind-induced vibrations in building structures. The results are promising and show viscous-damping walls are highly effective in most cases. The study provides evidence that viscous-damping walls are also effective in controlling cross-wind vibrations. This additional benefit is currently not considered when viscous-damping walls are designed and installed in actual buildings. At other angles of wind attack the viscous-damping action remained highly effective in suppressing wind-induced vibrations. It is hoped that this paper will spark interest in viscous-damping walls and encourage further research and development.

## Acknowledgements

This research was supported by the Research Grants Council of Hong Kong and the Committee on Research and Conference Grants of the University of Hong Kong. Their support is gratefully acknowledged.

## References

- Arima, F., M. Miyazaki, H. Tanaka and Y. Yamazaki (1988), "A study on buildings with large damping using viscous damping walls", *Proc. of Ninth World Conf. on Earthq. Eng.*, **V**, 821-826.
- Miyazaki, M. and Mitsusaka, Y. (1992), "Design of a building with 20% or greater damping", *Proc. of the Tenth World Conf. on Earthq. Eng.*, 4143-4148.
- Miyazaki, M., Y. Kitada, F. Arima and I. Hristov (1986), "Earthquake response control design of buildings using viscous damping walls," *Proc. Constr. of the First East Asian Conf. on Struct. Eng. and Const.*, 1882-1891.
- PSRG(Protective Systems Research Group of the Earthquake Engineering Research Center at the University of California at Berkeley), (1997), Buildings in Japan incorporating passive energy dissipation systems. URL: <http://www.eerc.berkeley.edu/prosys/japanpedbldgs.html>
- Yeung, N. (2000), "Viscous-damping walls for controlling wind-induced vibrations in buildings", Ph.D. Thesis, Department of Civil Engineering, The University of Hong Kong, Hong Kong SAR.
- Yeung, N. and Pan, A.D.E. (1997), "Viscous-damping wall and cladding as passive control for high-rise buildings", *Proc. of the 2nd European & African Conf. on Wind Eng.*, Genova, Italy, **II**, 1643-1650.
- Yeung, N. and Pan, A.D.E. (1998), "The effectiveness of viscous-damping walls for controlling wind vibrations in multi-story buildings", *J. Wind Eng. Ind. Aerod.*, **77&78**, 337-348.

## Notation

The following symbols are used in this paper :

$A$	effective area
$a$	$= 0.08 \times (1 + R_p) \times T^{(0.727-0.0206R_p)}$ , temperature coefficient
$a_m, a_p$	acceleration of model, prototype
$a_r$	$= \begin{cases} 1.221 \times e^{-0.4\gamma} (\gamma < 0.5) \\ 1.284 \times e^{-0.5\gamma} (\gamma \leq 0.5) \end{cases}$
	modification factor for displacement used in Eq. (5)
$dv$	relative velocity
$dy$	gap size between wall plates
$f$	frequency of vibration
$F_m / F_p$	force of model, prototype
$I_m / I_p$	moment of inertial of model, prototype
$J_m / J_p$	mass moment of inertia of model, prototype
$K$	$= 0.9 \times a \times \mu \times f^{0.5} \times A / dy$ , reference stiffness used in Eq. (5)
$K_m / K_p$	stiffness of model, prototype
$L_m, L_p$	standard length of model, prototype
$m_m / m_p$	mass of model, prototype
$M_m / M_p$	moment of model, prototype
$N_m / N_p$	frequency of model, prototype
$Q_c$	damping force
$Q_k$	restoring force
$Q_w$	viscous-resistant force generated in the viscous-damping wall
$R_p$	$= 96,600 / U_{p30}$ , viscous ratio
$T, t$	temperature of viscous fluid
$T_m, T_p$	time of model, prototype
$U_{p30}$	standard viscosity at reference temperature 30°C (poise) used in $R_p$
$v$	velocity
$V_m, V_p$	velocity of model, prototype
$\alpha, \beta$	exponent factor obtained from experiments
$\gamma$	$= \delta / dy$ , displacement gradient used in factor $a_r$
$\delta$	relative displacement between wall plates used in $\gamma$
$\rho_{air m} / \rho_{air p}$	air density around model, prototype
$\rho_m / \rho_p$	material density of model, prototype
$\mu$	viscosity of the viscous fluid
$\zeta_m / \zeta_p$	damping of model, prototype